

# A potential model prediction of fully-heavy tetraquarks $QQ\bar{Q}\bar{Q}$ ( $Q = c, b$ )

Gang Yang,<sup>1,2</sup> Jialun Ping,<sup>3</sup> Lianyi He,<sup>2,\*</sup> and Qing Wang<sup>2,†</sup>

<sup>1</sup>*Department of Physics, Zhejiang Normal University, Jinhua 321004, China*

<sup>2</sup>*Department of Physics, Tsinghua University, Beijing 100084, China*

<sup>3</sup>*Department of Physics, Nanjing Normal University, Nanjing 210023, China*

The fully-heavy tetraquark states  $QQ\bar{Q}\bar{Q}$  ( $Q = c, b$ ) are systematically investigated by means of a nonrelativistic potential model. The model is based on the lattice QCD study of the two-body  $Q\bar{Q}$  interaction, which exhibits a spin-independent Cornell potential along with a spin-spin interaction. The four-body problem is implemented with a highly accurate computation approach, the Gaussian expansion method. Both meson-meson and diquark-antidiquark configurations along with their couplings are considered for spin-parity quantum numbers  $J^P = 0^+, 1^+$ , and  $2^+$  in the iso-scalar sector  $I = 0$ . For the all-charm case, resonances with  $J^P = 0^+$  and  $1^+$  are located in the mass region 6.4 GeV–6.6 GeV. For  $J^P = 2^+$ , we find a resonance with mass around 7.0 GeV, which agrees well with the structure recently seen by the LHCb collaboration. For the all-bottom case, we find possible bound states with masses around 18.0 GeV and resonances with masses around 19.1 GeV. All these fully-heavy tetraquarks exhibit compact configurations, i.e., the distance between any two heavy quarks/antiquarks are around 0.3 fm for the all-charm case and around 0.2 fm for the all-bottom case.

## I. INTRODUCTION

With the development in high energy physics, large numbers of efforts contribute to the understanding of exotic multi-quark states composed of heavy flavors. In recent years, the LHCb collaboration announced five excited  $\Omega_c$  baryons in the  $\Xi_c^+ K^-$  mass spectrum [1] and four narrow excited  $\Omega_b$  baryons in the  $\Xi_b^0 K^-$  mass spectrum [2]. In 2019, they also discovered two excited bottom baryons,  $\Lambda_b^0(6146)$  and  $\Lambda_b^0(6152)$  [3]. Later on, one more excited  $\Lambda_b^0$  baryon around 6070 MeV in the  $\Lambda_b^0 \pi^+ \pi^-$  invariant mass spectrum was announced [4], consistent with the report by the CMS collaboration [5]. Additionally, three excited  $\Xi_c^0$  states were announced by the LHCb collaboration in the  $\Lambda_c^+ K^-$  mass spectrum [6]. All of these newly discovered exotic baryons are undoubtedly excellent supplements for the scarce data of heavy flavor baryons in PDG. Furthermore, these experimental findings also have triggered enormous theoretical investigations. Three-quark excited states of  $\Omega_c$  are suggested by QCD sum rules [7] and different potential models [8–10]. The P-wave  $\Omega_b$  states are preferred by potential model [11], heavy quark effective theory [12], QCD sum rules [13], and decay properties [14]. Meanwhile, the baryon-meson molecule picture is suggested for the excited  $\Omega_b$  baryons in Ref. [15]. With a QCD sum rules approach,  $\Lambda_b^0(6072)$ ,  $\Lambda_b^0(6146)$ , and  $\Lambda_b^0(6152)$  can be identified as the radial and angular excited bottom baryons [16–18]. Furthermore, 3-quark configurations of excited  $\Xi_c^0$  baryons are identified in the chiral quark model [19],  $^3P_0$  model [20] and QCD sum rules [21]. However, the  $\bar{D}\Lambda - \bar{D}\Sigma$  molecular states are also suggested by Ref. [22].

Apart from the heavy flavor baryons, exotic states *i.e.*, tetraquark and pentaquark states are also significant sectors in the contemporary hadronic physics. In 2015 and 2019, hidden-charm pentaquarks  $P_c^+(4380)$ ,  $P_c^+(4312)$ ,  $P_c^+(4440)$  and  $P_c^+(4457)$  were reported by the LHCb collaboration in the  $\Lambda_b^0$  decay,  $\Lambda_b^0 \rightarrow J/\psi K^- p$  [23, 24]. Moreover, during the past decade, more than two dozens of unconventional charmonium- and bottomonium-like states, the so-called XYZ mesons, have been observed at B-factories (BaBar, Belle and CLEO),  $\tau$ -charm facilities (CLEO-c and BESIII) and also proton-(anti)proton colliders (CDF, D0, LHCb, ATLAS and CMS), *e.g.*,  $Y(4260)$  discovered by the BaBar Collaboration in 2005 [25],  $Z^+(4430)$  discovered by the Belle Collaboration in 2007 [26],  $Y(4140)$  discovered by the CDF Collaboration in 2009 [27], and  $Z_c^+(3900)$  discovered by the BESIII Collaboration in 2013 [28], *etc.* Additionally, an extremely non-relativistic 4-body systems  $QQ\bar{Q}\bar{Q}$  are quite charming. The CMS collaboration has made the benchmark measurement of the  $\Upsilon(1S)$  pair production at the LHC  $pp$  collision at  $\sqrt{s}=8$  TeV [29], a subsequent preliminary investigation using CMS data shows an excess at 18.4 GeV in the  $\Upsilon\ell^+\ell^-$  decay channels [30–32]. This excess, if confirmed in the future data, could be a  $bb\bar{b}\bar{b}$  tetraquark state. Besides, a significant peak at  $\sim 18.2$  GeV was observed in Cu+Au collisions at RHIC [33]. However, no evidence has been provided from the LHCb collaboration by searching for the  $\Upsilon(1S)\mu^+\mu^-$  invariant mass spectrum [34]. Nevertheless, a new possible  $cc\bar{c}\bar{c}$  structure at 6.9 GeV was seen by the same collaboration [35]. Based on these facts, more investigations on the fully-heavy tetraquark states could be considered in future LHC experiment *e.g.*, ATLAS, CMS and LHCb.

The interpretations on these exotic states are carried out by various theoretical approaches. In particular, the three newly announced hidden-charm pentaquarks,  $P_c^+(4312)$ ,  $P_c^+(4440)$  and  $P_c^+(4457)$  are favored as the molecular states of  $\Sigma_c \bar{D}^*$  in effective field theory [36, 37],

\* lianyi@mail.tsinghua.edu.cn

† particle@mail.tsinghua.edu.cn

QCD sum rules [38], potential model [39–44], heavy quark spin multiplet structures [45, 46] and heavy hadron chiral perturbation theory [47] *etc.* Meanwhile, their decay properties [48] and photo-production process [49, 50] are discussed. As for the other types of pentaquarks, bound state for  $\bar{Q}qqqq$  system is unavailable in the study with a constituent model [51]. Several narrow double-heavy pentaquark states are obtained in the systematic investigations by potential models [52–54]. In one-boson-exchange model, possible triple-charm molecular pentaquarks  $\Xi_{cc}D^{(*)}$  are suggested [55].

Furthermore, extensive theoretical investigations devote to the tetraquark sector. Firstly, in double-heavy tetraquark states *e.g.*, in heavy quark limit, stable and extremely narrow  $bb\bar{u}\bar{d}$  tetraquark state with the  $J^P = 1^+$  must exist [56]. In Ref. [57] the predicted mass of  $bb\bar{u}\bar{d}$  state within the same spin-parity is  $10389 \pm 12$  MeV. Mass, lifetime and decay modes of this tetraquark are investigated in Ref. [58]. A compact double-bottom tetraquark state with  $IJ^P = 01^+$  is also presented in heavy-ion collisions at the LHC [59] and actually, in 1988 the dimeson  $T(bb\bar{u}\bar{d})$  had already been proposed [60]. Besides, a narrow  $(bb)(\bar{u}\bar{d})$  diquark-antidiquark state with  $IJ^P = 01^+$  is predicted in Ref. [61, 62]. A  $\bar{b}b\bar{u}d$  bound state also with  $IJ^P = 01^+$  is stable against the strong and electromagnetic decay and its mass is  $10476 \pm 24 \pm 10$  MeV by Lattice QCD [63], this deeply bound state is supported also by the same formalism in Refs. [64, 65]. Meanwhile, there are also QCD sum rules predicted a mass  $7105 \pm 155$  MeV for  $bc\bar{u}\bar{d}$  axial-vector tetraquark state [66], and  $I(J^P) = 0(1^+) ud\bar{c}\bar{d}$  tetraquark which binding energy is 15 to 61 MeV with respect to  $\bar{D}B^*$  threshold is proposed by Ref. [67]. Moreover, the production potential of double-heavy tetraquarks at a Tera-Z factory and the LHC are estimated [68, 69].

Secondly, in fully-heavy tetraquarks sector, debates on these extremely non-relativistic systems,  $QQ\bar{Q}\bar{Q}$  ( $Q = c, b$ ) are also very intensely: the existence of  $bb\bar{b}\bar{b}$  bound state is supported by phenomenological model calculation [70–73], QCD sum rules [74, 75], and diffusion Monte Carlo method [76]. The decay property of was also studied in Ref. [77] with a conclusion that fully-bottom in  $2^+$  state maybe possible. A narrow  $cc\bar{c}\bar{c}$  tetraquark state in the mass region 5 – 6 GeV has been predicted by the Bethe-Salpeter approach [78] and also in several phenomenological models [70, 79–81]. Furthermore, searching for the fully-heavy tetraquark states are valuable theoretically [82]. However, there are still intense debates on the observation of these exotic states. No  $cc\bar{c}\bar{c}$  and  $bb\bar{b}\bar{b}$  bound states can be formed within effective model calculations [83, 84, 86–89] and lattice QCD [90], but possible stable or narrow states in the  $bb\bar{b}\bar{c}$  and  $bcb\bar{c}$  systems [83, 84]. Recently, P-wave fully-heavy tetraquarks are investigated by means of a non-relativistic potential quark model [85].

We study herein, with a complex scaling range of potential model formalism which is based on the results of Lattice QCD investigations on the interaction of heavy

quark pair, the possibility of having tetraquark bound- and resonance-states in the fully-heavy sector with quantum numbers  $J^P = 0^+, 1^+$  and  $2^+$ , and in the 0 isospin sectors. Two configurations, meson-meson and diquark-antidiquark structures along with their couplings are all considered for each quantum states. The bound and resonance states, if possible, their internal structures and components in the complete coupled-channels calculation are analyzed by computing the distances among any pair of quarks and the contributions of each channel’s wave functions.

The 4-body bound state problem is implemented by two strong foundations, the Gaussian expansion method (GEM) [92] which has been demonstrated to be accurate as a Faddeev calculation (see, for instance, Figs. 15 and 16 of Ref. [92]), and a reliable potential for heavy quark sectors ( $Q = c, b$ ) according to the Lattice study [93]. Meanwhile, a powerful technique, complex scaling method (CSM) is also employed as our previous studies on the double-heavy tetraquarks [62] and the double-charm pentaquarks [54]. In this formalism, the bound, resonance and scattering states can all be described simultaneously.

The structure of this paper is organized in the following way. In Sec. II theoretical framework which includes the potential model and  $QQ\bar{Q}\bar{Q}$  tetraquark wave-functions is briefly presented and discussed. Section III is devoted to the analysis and discussion on the obtained results of  $QQ\bar{Q}\bar{Q}$  in each quantum states. The summary are presented in Sec. IV.

## II. THEORETICAL FRAMEWORK

In the extremely non-relativistic systems  $QQ\bar{Q}\bar{Q}$  ( $Q = c, b$ ), the interaction between a heavy quark and a heavy antiquark can be well approximated by the Cornell potential along with a spin-spin interaction according to the Lattice QCD investigation [93]. Generally, this concise fact can be incorporated into the following form of four-body Hamiltonian,

$$H = \sum_{i=1}^4 \left( m_i + \frac{\vec{p}_i^2}{2m_i} \right) - T_{\text{CM}} + \sum_{j>i=1}^4 V(\vec{r}_{ij}), \quad (1)$$

where the center-of-mass kinetic energy  $T_{\text{CM}}$  is subtracted without losing a generality since we mainly focus on the internal relative motions of multi-quark system. Interaction part is of two-body potential which reads

$$V_{Q\bar{Q}}(\vec{r}_{ij}) = -\frac{\alpha}{\vec{r}_{ij}} + \sigma\vec{r}_{ij} + \beta e^{-\vec{r}_{ij}}(\vec{s}_i \cdot \vec{s}_j), \quad (2)$$

and includes the coulomb, linear confinement and spin-spin interactions. Meanwhile, the quark-quark interaction  $V_{QQ}$  is half of  $V_{Q\bar{Q}}$  according to the quark model and lattice QCD investigations [94]. Table I listed the values of model parameters according to Ref. [95]. Additionally, the calculated masses of S-wave  $Q\bar{Q}$  mesons

TABLE I. Model parameters.

Quark masses	$m_c$ (MeV)	1290
	$m_b$ (MeV)	4700
Coulomb	$\alpha$	0.4105
Confinement	$\sigma$ (GeV <sup>2</sup> )	0.2
Spin-Spin	$\gamma$ (GeV)	1.982
	$\beta_c$ (GeV)	2.06
	$\beta_b$ (GeV)	0.318

TABLE II. Theoretical and experimental masses of the S-wave  $QQ\bar{Q}\bar{Q}$  mesons, unit in MeV.

State	$M_{th}$	$M_{exp}$
$\eta_c(1S)$	2968	2981
$\eta_c(2S)$	3655	3639
$J/\psi(1S)$	3102	3097
$\psi(2S)$	3720	3686
$\eta_b(1S)$	9401	9398
$\eta_b(2S)$	9961	9999
$\Upsilon(1S)$	9463	9460
$\Upsilon(2S)$	9981	10023

along with their experimental values are listed in Table II. Obviously, these theoretical masses are nicely consistent with the experimental data and will be useful in identifying the possible bound and resonance states in  $QQ\bar{Q}\bar{Q}$  tetraquark sectors.

Furthermore, as to have a better classification of the bound, resonance and scattering states in  $QQ\bar{Q}\bar{Q}$  states, the complex scaling method is employed. In particular, the coordinates of relative motions between quarks in Eq. (1) are transformed with a complex rotation,  $\vec{r} \rightarrow \vec{r}e^{i\theta}$ . Hence, the four-body systems are solved in a complex scaled Schrödinger equation:

$$[H(\theta) - E(\theta)] \Psi_{JM}(\theta) = 0 \quad (3)$$

The above solved complex energy could be classified into three kinds of poles (bound, resonance and scattering states) in a complex energy plane according to the so-called ABC theorem [96, 97]. Especially, the bound state and resonance pole is stable and independent of the rotated angle  $\theta$ . However, the continuum state is just aligned along the cut line with a  $2\theta$  rotated angle. More details on CSM in hadronic physics can be referenced in Ref. [54, 62].

There are four fundamental degrees of freedom in quark level. Namely, color, flavor, spin and space which are generally accepted in the QCD theory and the multi-quark system wave function is a product of them. Fig. 1 shows two kinds of configurations for fully-heavy tetraquarks  $QQ\bar{Q}\bar{Q}$  ( $Q = c, b$ ). In particular, Fig. 1(a) is

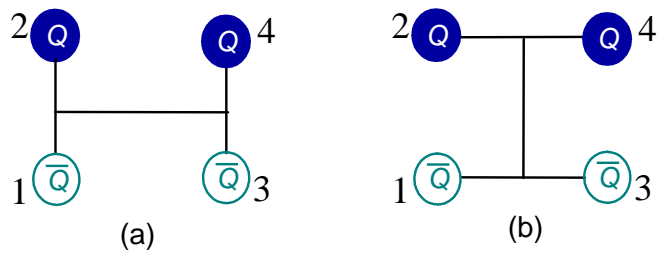


FIG. 1. Two types of configurations in fully-heavy tetraquarks. Panel (a) is meson-meson structure and panel (b) is diquark-antidiquark one. ( $Q = c, b$ )

the meson-meson structure and diquark-antidiquark one is of Fig. 1(b), both of them and their coupling are considered in our investigation. However, this is not an unique way because the authors of Refs. [98, 99] assert that it is enough to consider the color singlet channel when all possible excited states of a system are included. After a comparison, a more economical way of computing by considering all of the possible configurations and their couplings is preferred. Although the effect of identical particles exchange in these two configurations will lead to a singular matrix when diagonalize the hamiltonian. To solve the double counting problem, the eigenfunction method is employed. Firstly, the overlap matrix is diagonalized, and the eigenvectors with eigenvalue 0 are abandoned, then we re-construct the hamiltonian matrix by using the remained eigenvectors. At last, the new hamiltonian matrix is diagonalized to obtained the energies of the system.

Firstly, for the color degree-of-freedom, much more richer structures in multi-quark system will be discussed than conventional hadrons ( $q\bar{q}$  mesons and  $qqq$  baryons). Both color-singlet (two color-singlet clusters coupling,  $1 \times 1$ ) and hidden-color (two color-octet clusters coupling,  $8 \times 8$ ) channels in meson-meson configuration of Fig. 1(a) are considered. Their wave functions are signed as  $\chi_1^c$  and  $\chi_2^c$ , respectively.

$$\chi_1^c = \frac{1}{3}(\bar{r}r + \bar{g}g + \bar{b}b) \times (\bar{r}r + \bar{g}g + \bar{b}b), \quad (4)$$

$$\begin{aligned} \chi_2^c = & \frac{\sqrt{2}}{12}(3\bar{b}r\bar{r}b + 3\bar{g}r\bar{r}g + 3\bar{b}g\bar{g}b + 3\bar{g}b\bar{b}g + 3\bar{r}g\bar{g}r \\ & + 3\bar{r}b\bar{b}r + 2\bar{r}r\bar{r}r + 2\bar{g}g\bar{g}g + 2\bar{b}b\bar{b}b - \bar{r}r\bar{g}g \\ & - \bar{g}g\bar{r}r - \bar{b}b\bar{g}g - \bar{b}b\bar{r}r - \bar{g}g\bar{b}b - \bar{r}r\bar{b}b). \end{aligned} \quad (5)$$

Besides, also according to an increased sequence of numbers signed in Fig. 1, the color wave functions of diquark-antidiquark configuration shown in Fig. 1(b) are  $\chi_3^c$  (color triplet-antitriplet clusters coupling,  $3 \times \bar{3}$ ) and  $\chi_4^c$  (color

sxtet-antisxtet clusters coupling,  $6 \times \bar{6}$ ), respectively:

$$\begin{aligned} \chi_3^c = & \frac{\sqrt{3}}{6} (\bar{r}r\bar{g}g - \bar{g}r\bar{r}g + \bar{g}g\bar{r}r - \bar{r}g\bar{g}r + \bar{r}r\bar{b}b \\ & - \bar{b}r\bar{r}b + \bar{b}b\bar{r}r - \bar{r}b\bar{b}r + \bar{g}g\bar{b}b - \bar{b}g\bar{g}b \\ & + \bar{b}b\bar{g}g - \bar{g}b\bar{b}g), \end{aligned} \quad (6)$$

$$\begin{aligned} \chi_4^c = & \frac{\sqrt{6}}{12} (2\bar{r}r\bar{r}r + 2\bar{g}g\bar{g}g + 2\bar{b}b\bar{b}b + \bar{r}r\bar{g}g + \bar{g}r\bar{r}g \\ & + \bar{g}g\bar{r}r + \bar{r}g\bar{g}r + \bar{r}r\bar{b}b + \bar{b}r\bar{r}b + \bar{b}b\bar{r}r \\ & + \bar{r}b\bar{b}r + \bar{g}g\bar{b}b + \bar{b}g\bar{g}b + \bar{b}b\bar{g}g + \bar{g}b\bar{b}g). \end{aligned} \quad (7)$$

However, one can notice that there is no color-depended interaction in the potential of Eq. (2). Therefore, the matrix elements of these basis in color degree-of-freedom will be identity.

Secondly, as for the flavor degree-of-freedom, since we are dealing with fully-heavy tetraquarks, only the isoscalar  $I = 0$  sector will be considered. The flavor wavefunctions signed as  $\chi_{I,M_I}^{f_i}$  with the superscript  $i = 1$  and  $2$  are of  $cc\bar{c}\bar{c}$  and  $bb\bar{b}\bar{b}$  systems, respectively. The details are trivial,

$$\chi_{0,0}^{f_1} = \bar{c}c\bar{c}c, \quad \chi_{0,0}^{f_2} = \bar{b}b\bar{b}b. \quad (8)$$

Four-quark systems with total spin  $S$  ranging from 0 to 2 are all studied in this work. Meanwhile, due to there is not any spin-orbital coupling dependent potential included in the Hamiltonian, the third component ( $M_S$ ) of tetraquark spin can be assumed to be equal to the total one without loss of generality too. Then the spin wave functions  $\chi_{S,M_S}^\sigma$  are given by:

$$\chi_{0,0}^{\sigma_1}(4) = \chi_{00}^\sigma \chi_{00}^\sigma \quad (9)$$

$$\chi_{0,0}^{\sigma_2}(4) = \frac{1}{\sqrt{3}} (\chi_{11}^\sigma \chi_{1,-1}^\sigma - \chi_{10}^\sigma \chi_{10}^\sigma + \chi_{1,-1}^\sigma \chi_{11}^\sigma) \quad (10)$$

$$\chi_{1,1}^{\sigma_1}(4) = \chi_{00}^\sigma \chi_{11}^\sigma \quad (11)$$

$$\chi_{1,1}^{\sigma_2}(4) = \chi_{11}^\sigma \chi_{00}^\sigma \quad (12)$$

$$\chi_{1,1}^{\sigma_3}(4) = \frac{1}{\sqrt{2}} (\chi_{11}^\sigma \chi_{10}^\sigma - \chi_{10}^\sigma \chi_{11}^\sigma) \quad (13)$$

$$\chi_{2,2}^{\sigma_1}(4) = \chi_{11}^\sigma \chi_{11}^\sigma \quad (14)$$

these expressions are obtained by considering the coupling of two sub-clusters spin wave functions with SU(2) algebra, and the necessary bases are read as

$$\chi_{11}^\sigma = \alpha\alpha, \quad \chi_{1,-1}^\sigma = \beta\beta \quad (15)$$

$$\chi_{10}^\sigma = \frac{1}{\sqrt{2}} (\alpha\beta + \beta\alpha) \quad (16)$$

$$\chi_{00}^\sigma = \frac{1}{\sqrt{2}} (\alpha\beta - \beta\alpha) \quad (17)$$

The 4-body bound state equation are solved by means of an exact and high efficiency numerical approach, Gaussian expansion method [92]. Three relative motions of

4-quark systems are all expanded with Gaussian basis whose widths are taken as the geometric progression sizes<sup>1</sup> and the orbital form is

$$\phi_{nlm}(\vec{r}e^{i\theta}) = N_{nl}(re^{i\theta})^l e^{-\nu_n(re^{i\theta})^2} Y_{lm}(\hat{r}). \quad (18)$$

Since our present study concentrates on the  $S$ -wave state of fully-heavy tetraquarks, the value of spherical harmonic function is just a constant *i.e.*,  $Y_{00} = \sqrt{1/4\pi}$ . Eq. (19) shows the general spatial wave function of tetraquark states:

$$\psi_{LM_L}(\theta) = \left[ \left[ \phi_{n_1 l_1}(\vec{\rho}e^{i\theta}) \phi_{n_2 l_2}(\vec{\lambda}e^{i\theta}) \right]_l \phi_{n_3 l_3}(\vec{R}e^{i\theta}) \right]_{LM_L}, \quad (19)$$

where the internal Jacobi coordinates for Fig. 1(a) of meson-meson configuration are defined as

$$\vec{\rho} = \vec{x}_1 - \vec{x}_2, \quad (20)$$

$$\vec{\lambda} = \vec{x}_3 - \vec{x}_4, \quad (21)$$

$$\vec{R} = \frac{m_1 \vec{x}_1 + m_2 \vec{x}_2}{m_1 + m_2} - \frac{m_3 \vec{x}_3 + m_4 \vec{x}_4}{m_3 + m_4}, \quad (22)$$

and the diquark-antidiquark structure of Fig. 1(b) are,

$$\vec{\rho} = \vec{x}_1 - \vec{x}_3, \quad (23)$$

$$\vec{\lambda} = \vec{x}_2 - \vec{x}_4, \quad (24)$$

$$\vec{R} = \frac{m_1 \vec{x}_1 + m_3 \vec{x}_3}{m_1 + m_3} - \frac{m_2 \vec{x}_2 + m_4 \vec{x}_4}{m_2 + m_4}. \quad (25)$$

Obviously, with these sets of coordinates the center-of-mass kinetic term  $T_{CM}$  can be completely eliminated for a nonrelativistic system. Additionally, the complex scaling angle  $\theta$  are employed in the Jacobi coordinates of Eq. (19).

Finally, the complete wave-function which fulfill the Pauli principle is written as

$$\Psi_{JM_J, I, i, j, k}(\theta) = \mathcal{A} \left[ [\psi_L(\theta) \chi_S^{\sigma_i}(4)]_{JM_J} \chi_I^{f_j} \chi_k^c \right], \quad (26)$$

where  $\mathcal{A}$  is the antisymmetry operator of fully-heavy tetraquarks by considering the nature of identical particle interchange ( $QQ$  and  $\bar{Q}\bar{Q}$ ). This is necessary since the complete wave function of the 4-quark system is constructed from two sub-clusters, *i.e.*, meson-meson and diquark-antidiquark structures. Particularly, the definitions of these two configurations in Fig. 1 with the quark arrangements of  $\bar{Q}Q\bar{Q}Q$  are both

$$\mathcal{A} = 1 - (13) - (24) + (13)(24). \quad (27)$$

### III. RESULTS

The low-lying  $S$ -wave states of fully-heavy tetraquarks  $QQ\bar{Q}\bar{Q}$  ( $Q = c, b$ ) are systematically investigated in the

<sup>1</sup> The details on Gaussian parameters can be found in Ref. [91]

TABLE III. All possible channels for  $cc\bar{c}\bar{c}$  and  $bb\bar{b}\bar{b}$  tetraquark systems. The second column shows the necessary basis combination in spin ( $\chi_J^{\sigma_i}$ ), flavor ( $\chi_I^{f_j}$ ) and color ( $\chi_k^c$ ) degrees of freedom. Particularly, the flavor indices ( $j$ ) 1 and 2 are of  $cc\bar{c}\bar{c}$  and  $bb\bar{b}\bar{b}$ , respectively.

$IJ^P$	Index	$\chi_J^{\sigma_i}; \chi_I^{f_j}; \chi_k^c$ [ $i; j; k$ ]	Channel
$00^+$	1	[1; 1(2); 1]	$\eta_c\eta_c; \eta_b\eta_b$
	2	[2; 1(2); 1]	$J/\psi J/\psi; \Upsilon\Upsilon$
	3	[1; 1(2); 4]	$(cc)(\bar{c}\bar{c}); (bb)(\bar{b}\bar{b})$
	4	[2; 1(2); 3]	$(cc)^*(\bar{c}\bar{c})^*; (bb)^*(\bar{b}\bar{b})^*$
$01^+$	1	[1; 1(2); 1]	$\eta_c J/\psi; \eta_b \Upsilon$
	2	[3; 1(2); 1]	$J/\psi J/\psi; \Upsilon\Upsilon$
	3	[3; 1(2); 3]	$(cc)^*(\bar{c}\bar{c})^*; (bb)^*(\bar{b}\bar{b})^*$
$02^+$	1	[1; 1(2); 1]	$J/\psi J/\psi; \Upsilon\Upsilon$
	2	[1; 1(2); 3]	$(cc)^*(\bar{c}\bar{c})^*; (bb)^*(\bar{b}\bar{b})^*$

potential model which is based on the results of Lattice QCD investigation on the two-body interaction  $V_{Q\bar{Q}}$ . All possible meson-meson and diquark-antidiquark structures for  $cc\bar{c}\bar{c}$  and  $bb\bar{b}\bar{b}$  systems which fulfill the Pauli principle are listed in Table III. In particular, the third column shows the necessary basis combination in spin ( $\chi_J^{\sigma_i}$ ), flavor ( $\chi_I^{f_j}$ ), and color ( $\chi_k^c$ ) degrees-of-freedom. The physical channels with dimeson and diquark-antidiquark configurations are listed in the last column. Besides, all of those possible channels in one certain quantum state are numbered in the first column.

Tables range from IV to XVIII summarized our calculated results (mass, size and component) of possible low-lying fully-heavy tetraquarks. Particularly, for the  $cc\bar{c}\bar{c}$  tetraquarks, Tables IV, VII and IX list the calculated resonance mass of each channel along with their coupled results in  $0^+$ ,  $1^+$  and  $2^+$  states, respectively. The component and inner structure which is the distance among any quark pair of these resonances are listed in Table V, VI for  $0^+$  state, Table VIII for  $1^+$  state and Table X for  $2^+$  state, respectively. These results can reveal the nature of  $QQ\bar{Q}\bar{Q}$  systems we are dealing with. Meanwhile, the fully-bottom sectors can be referenced in Tables ranging from XI to XVII where results both on available bound and resonance states are listed. Then an organized results on the obtained exotic states of fully-heavy tetraquarks are summarized in Table XVIII.

Additionally, the distributions of complex energies of these fully-heavy tetraquarks in the complete coupled-channels calculation by complex scaling method are presented from Fig. 2 to 7. In each figures, the transverse direction is of the real part of complex energy  $E$  which stands for the mass of tetraquarks, and the longitudinal one is the imaginary part of  $E$  which is related to the width,  $\Gamma = -2Im(E)$ .

TABLE IV. Possible resonance states of fully-charm tetraquarks with quantum numbers  $IJ^P = 00^+$ . The first column shows the allowed channels and, in the parenthesis, the noninteracting meson-meson threshold values. Meson-meson and diquark-antidiquark channels are indexed in the second column respectively, the last column refers to the theoretical mass of each channels and their couplings, unit in MeV.

Channel	Index	$M$
$\eta_c\eta_c(5936)$	1	6536
$J/\psi J/\psi(6204)$	2	6657
$(cc)(\bar{c}\bar{c})$	3	6683
$(cc)^*(\bar{c}\bar{c})^*$	4	6469
Mixed		6449 <sup>1st</sup> 6659 <sup>2nd</sup>

TABLE V. Component of each channel in the coupled-channels calculation of fully-charm resonance states with  $IJ^P = 00^+$ .

	$\eta_c\eta_c$	$J/\psi J/\psi$	$(cc)(\bar{c}\bar{c})$	$(cc)^*(\bar{c}\bar{c})^*$
1st	6.6%	2.4%	0.9%	90.1%
2nd	4.4%	25.2%	69.2%	1.2%

TABLE VI. The distances, between any two quarks of the found fully-charm resonance states with  $IJ^P = 00^+$  in coupled-channels calculation, unit in fm.

	$r_{cc}$	$r_{c\bar{c}}$	$r_{\bar{c}\bar{c}}$
1st	0.340	0.324	0.340
2nd	0.352	0.343	0.352

In the following parts we will describe the details of theoretical investigations on each sector of fully-heavy tetraquarks.

### A. fully-charm tetraquarks

In the fully-charm  $cc\bar{c}\bar{c}$  sector, no bound state is obtained for all of the three  $J^P = 0^+$ ,  $1^+$  and  $2^+$  quantum states. However, several resonance states are available and let us discuss them individually.

**The  $I(J^P) = 0(0^+)$  channel:** There are both two channels for the meson-meson and diquark-antidiquark configurations, namely  $\eta_c\eta_c$ ,  $J/\psi J/\psi$ ,  $(cc)(\bar{c}\bar{c})$  and  $(cc)^*(\bar{c}\bar{c})^*$ . In Table IV one could notice that the theoretical threshold values of 5936 MeV for  $\eta_c\eta_c$  and 6204 MeV for  $J/\psi J/\psi$  are quite comparable with the experimental data 5962 MeV and 6194 MeV, respectively. Firstly, in each single channel calculation, no bound state is found neither in the dimeson channels nor the

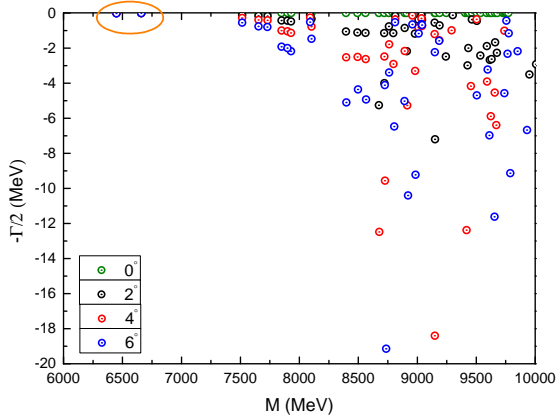


FIG. 2. Complex energies of fully-charm tetraquarks with  $IJ^P = 00^+$  in the coupled channels calculation,  $\theta$  varying from  $0^\circ$  to  $6^\circ$ .

diquark-antidiquark ones. However, resonance states above the lowest threshold  $\eta_c\eta_c(5936) \sim 600$  MeV are obtained. Particularly, in the  $\eta_c\eta_c$  and  $J/\psi J/\psi$  channels, we find two resonance whose masses are 6536 MeV and 6657 MeV, respectively. Besides, two more resonances within the similar mass region are obtained in  $(cc)(\bar{c}\bar{c})$  and  $(cc)^*(\bar{c}\bar{c})^*$  channels. The specific values are 6683 MeV and 6469 MeV, respectively.

In a further step which the complete coupled channels calculation is performed, and two resonance states with masses of 6449 MeV and 6659 MeV are found. Obviously, the coupled energy of the lower state 6449 MeV is near the  $(cc)^*(\bar{c}\bar{c})^*$  channel's 6469 MeV and the higher one is almost degenerate with  $J/\psi J/\psi$  channel. These features are supported by the presented results on the components of each channels of resonance states in Table V. For the first resonance state, 90% is of diquark-antidiquark channel  $(cc)^*(\bar{c}\bar{c})^*$  and the second one is  $\sim 70\%$   $(cc)(\bar{c}\bar{c})$  component. Hence the nature of compact structures of diquark-antidiquark channels are confirmed in Table VI which the distances for any pair of quarks are calculated. In particular, the sizes of these two resonance states are both around 0.34 fm, only the higher resonance state is a tiny larger  $\sim 0.1$  fm.

Fig. 2 shows the distributions of complex energies of  $cc\bar{c}\bar{c}$  system with  $0^+$  quantum numbers in the complete coupled-channels calculation by CSM. Generally, in the mass region from 7.5 GeV to 10.0 GeV the energy dots are unstable and always descend when the rotated angle  $\theta$  varied from  $0^\circ$  to  $6^\circ$ . This can be identified as the nature of scattering state. However, as the resonance masses presented in Table IV, two resonance poles circled with orange in Fig. 2 are independent of the complex angle  $\theta$  and fixed at 6.45 GeV and 6.66 GeV, respectively. Accordingly, these two resonance states are stable against the strong decay and expected to be confirmed experimentally.

TABLE VII. Possible resonance states of fully-charm tetraquarks with quantum numbers  $IJ^P = 01^+$ . The first column shows the allowed channels and, in the parenthesis, the noninteracting meson-meson threshold values. Meson-meson and diquark-antidiquark channels are indexed in the second column respectively, the last column refers to the theoretical mass of each channels and their couplings, unit in MeV. The component of each channels are listed in the last row.

Channel	Index	$M$
$\eta_c J/\psi(6070)$	1	6671
$(cc)^*(\bar{c}\bar{c})^*$	3	6674
Mixed		6657
Component (1; 3):	7.4%; 92.6%	

TABLE VIII. The distances, between any two quarks of the found fully-charm resonance states with  $IJ^P = 01^+$  in coupled-channels calculation, unit in fm.

$r_{cc}$	$r_{c\bar{c}}$	$r_{\bar{c}\bar{c}}$
0.356	0.341	0.356

**The  $I(J^P) = 0(1^+)$  channel:** Bound state is still unavailable in this sector, however, resonance states  $\sim 6.6$  GeV are found. Table VII presents two almost degenerate resonance states whose masses are 6671 MeV and 6674 MeV, respectively in the single channel calculations for meson-meson configuration  $\eta_c J/\psi$  and diquark-antidiquark one  $(cc)^*(\bar{c}\bar{c})^*$ . However, the  $J/\psi J/\psi$  channel listed in Table III is of scattering state. By comparing the  $\eta_c J/\psi$  threshold value which is 6070 MeV with the obtained resonance mass at 6671 MeV, a similar result as that in  $0^+$  case can be concluded that  $\sim 0.6$  GeV excitation energy region is quite possible for the existence of hadronic resonance state.

In additional, with a fully channels coupling which includes the  $\eta_c J/\psi$  and  $(cc)^*(\bar{c}\bar{c})^*$  configurations, a lower resonance mass 6657 MeV is obtained. Furthermore, the majority contributions ( $\sim 93\%$ ) come from the later channel,  $(cc)^*(\bar{c}\bar{c})^*$ . This resonance state can also be classified as compact tetraquark state owing to the calculated sizes of any pair of quarks are less than 0.36 fm in Table VIII.

When the complex scaling method is employed in the coupled-channels computation one could find that apart from one fixed resonance pole within the big orange circle is still at 6657 MeV of Fig. 3, the other higher excited states are all of the nature of scattering. This resonance mass is extremely close to 6659 MeV of the one obtained in  $0^+$  state and can be confirmed in future experiment.

**The  $I(J^P) = 0(2^+)$  channel:** Table IX lists one meson-meson  $J/\psi J/\psi$  channel and one diquark-antidiquark  $(cc)^*(\bar{c}\bar{c})^*$  channel, again the obtain resonance masses of them are degenerate with only 4 MeV

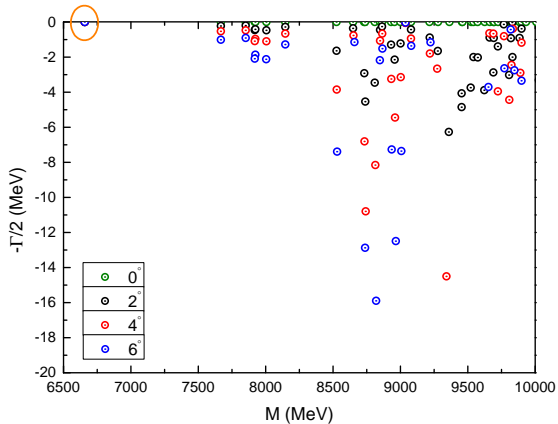


FIG. 3. Complex energies of fully-charm tetraquarks with  $IJ^P = 01^+$  in the coupled channels calculation,  $\theta$  varying from  $0^\circ$  to  $6^\circ$ .

difference. Besides, they are both around 7.0 GeV in this highest spin tetraquark state. Then in a two channels coupled-calculation, the lowest resonance mass (7022 MeV) depressed several MeV, and the components of  $J/\psi J/\psi$  and  $(cc)^*(\bar{c}\bar{c})^*$  are comparable with their percentages are about 40% and 60%, respectively. Although this resonance is found above the  $J/\psi J/\psi$  threshold value by 830 MeV, the nature of compact structure is still presented in Table X. Particularly, the calculated distances of any two quarks of  $cc\bar{c}\bar{c}$  state are  $\sim 0.38$  fm which is the same level as a conventional  $q\bar{q}$  meson.

Fig. 4 presents the calculated complex energies of  $cc\bar{c}\bar{c}$  tetraquarks in coupled-channels study. With the rotated angle  $\theta$  also varied from  $0^\circ$  to  $6^\circ$ , the obtained resonance state is fixed in the orange circle with mass of 7022 MeV. As a matter of fact, the mass of this  $02^+$  resonance state is consistent with the mass of structure reported by the LHCb collaboration recently [35], hence future measurements are needed to investigate if the structure is a new exotic state with compact configuration.

## B. fully-bottom tetraquarks

In the  $b\bar{b}b\bar{b}$  tetraquark sector, both bound and resonance for each  $J^P=0^+, 1^+$  and  $2^+$  iso-scalar states are found. Meanwhile, these exotic states are much more compact than the ones in fully-charm sector.

**The  $I(J^P) = 0(0^+)$  channel:** There are two di-meson channels  $\eta_b\eta_b$  and  $\Upsilon\Upsilon$ , two diquark-antidiquark channels  $(bb)(\bar{b}\bar{b})$  and  $(bb)^*(\bar{b}\bar{b})^*$  listed in Table XI. Firstly, in each single channel calculation, two low-lying exotic states are found for all of these four structures. Particularly, four bound states whose masses are 17999 MeV, 18038 MeV, 18068 MeV and 17975 MeV respectively are obtained for  $\eta_b\eta_b$ ,  $\Upsilon\Upsilon$ ,  $(bb)(\bar{b}\bar{b})$  and  $(bb)^*(\bar{b}\bar{b})^*$  channels.

TABLE IX. Possible resonance states of fully-charm tetraquarks with quantum numbers  $IJ^P = 02^+$ . The first column shows the allowed channels and, in the parenthesis, the noninteracting meson-meson threshold values. Meson-meson and diquark-antidiquark channels are indexed in the second column respectively, the last column refers to the theoretical mass of each channels and their couplings, unit in MeV. The component of each channels are listed in the last row.

Channel	Index	$M$
$J/\psi J/\psi(6204)$	1	7030
$(cc)^*(\bar{c}\bar{c})^*$	2	7026
Mixed		7022
Component (1; 2):		41.4%; 58.6%

TABLE X. The distances, between any two quarks of the found fully-charm resonance states with  $IJ^P = 02^+$  in coupled-channels calculation, unit in fm.

$r_{cc}$	$r_{c\bar{c}}$	$r_{\bar{c}\bar{c}}$
0.389	0.375	0.389

The binding energies are about 0.8 GeV to 0.9 GeV when compared with the lowest threshold value of  $\eta_b\eta_b(18802)$ . Furthermore,  $\sim 0.2$  GeV above this threshold line, we also find four stable resonance states and their masses are around 19.03 GeV. Among all of these four channels, masses of the bound and resonance states in  $(bb)^*(\bar{b}\bar{b})^*$  configuration is the lowest.

In a complete coupled-channels computation, two bound states with mass of 17955 MeV and 18030 MeV along with two resonances at 19005 MeV and 19049 MeV are obtained. Obviously, mass of the lower bound state is very close to  $(bb)^*(\bar{b}\bar{b})^*$  calculated mass (17975 MeV) and another bound one is both near  $\Upsilon\Upsilon$  and  $(bb)(\bar{b}\bar{b})$  channels. This feature also applies to the resonance states, since we can focus on the data in Table XII and XIII where the component of each channel and the inner structure of  $b\bar{b}b\bar{b}$  tetraquarks are presented in the complete coupled-channels calculation.

For the four listed exotic states in Table XII and XIII, the first two are of the bound states and the later two are of the resonances in a fully coupled-channels study. More than 70% components are contributed to the diquark-antidiquark channels,  $(bb)(\bar{b}\bar{b})$  or  $(bb)^*(\bar{b}\bar{b})^*$  for both bound and resonance states. However, the percentages of  $\eta_b\eta_b$  and  $\Upsilon\Upsilon$  channels do not exceed 25%. The calculated distances between any two quarks are smaller than fully-charm sector. They are all less than 0.27 fm, and in particular,  $\sim 0.16$  fm for bound states. These much more compact configurations are reasonable according to previous results on fully-charm sector.

Fig. 5 presents the results in complex range investigation. Clearly, with a rotated angle  $\theta$  varied in  $0^\circ - 6^\circ$

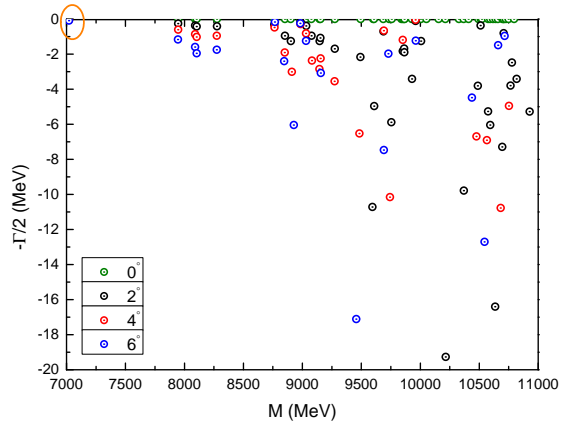


FIG. 4. Complex energies of fully-charm tetraquarks with  $IJ^P = 02^+$  in the coupled channels calculation,  $\theta$  varying from  $0^\circ$  to  $6^\circ$ .

TABLE XI. Possible bound and resonance states of fully-bottom tetraquarks with quantum numbers  $IJ^P = 00^+$ . The first column shows the allowed channels and, in the parenthesis, the noninteracting meson-meson threshold values. Meson-meson and diquark-antidiquark channels are indexed in the second column respectively, the third column refers to the theoretical mass of each channels and their couplings, binding energies of the dimeson channels are listed in the last column, unit in MeV.

Channel	Index	$M$	$E_b$
$\eta_b\eta_b(18802)$	1	$17999^{1st}$	-803
		$19036^{2nd}$	+234
$\Upsilon\Upsilon(18926)$	2	$18038^{1st}$	-888
		$19069^{2nd}$	+143
$(bb)(\bar{b}\bar{b})$	3	$18068^{1st}$	
		$19097^{2nd}$	
$(bb)^*(\bar{b}\bar{b})^*$	4	$17975^{1st}$	
		$19033^{2nd}$	
Mixed		$17955^{1st}$	
		$18030^{2nd}$	
		$19005^{3rd}$	
		$19049^{4th}$	

region, the two bound states and two resonance ones are always fixed in the complex plane. However, the other higher excited states are of the scattering nature.

**The  $I(J^P) = 0(1^+)$  channel:** In analogy with the  $cc\bar{c}\bar{c}$  tetraquarks in  $1^+$  state,  $\Upsilon\Upsilon$  channels are still of the scattering nature. However, bound and resonance states are available in  $\eta_b\Upsilon$  and  $(bb)^*(\bar{b}\bar{b})^*$  channels. They are located in the similar energy region as those  $bb\bar{b}\bar{b}$  tetraquarks with  $0^+$  quantum numbers. From Table XIV one can see it clearly that two almost degenerate states

TABLE XII. Component of each channel in the coupled-channels calculation of fully-bottom bound and resonance states with  $IJ^P = 00^+$ .

	$\eta_b\eta_b$	$\Upsilon\Upsilon$	$(bb)(\bar{b}\bar{b})$	$(bb)^*(\bar{b}\bar{b})^*$
1st	13.0%	5.2%	0.7%	81.1%
2nd	5.8%	23.5%	70.5%	0.2%
3rd	22.3%	6.7%	3.0%	68.0%
4th	9.4%	18.9%	70.7%	1.0%

TABLE XIII. The distances, between any two quarks of the found fully-bottom bound and resonance states with  $IJ^P = 00^+$  in coupled-channels calculation, unit in fm.

	$r_{bb}$	$r_{\bar{b}\bar{b}}$	$r_{\bar{b}b}$
1st	0.166	0.159	0.166
2nd	0.168	0.162	0.168
3rd	0.262	0.242	0.262
4th	0.264	0.246	0.264

for bound and resonance cases are obtained in these two configurations. Specifically, the bound states with masses of 18062 MeV and 18065 MeV are found in  $\eta_b\Upsilon$  and  $(bb)^*(\bar{b}\bar{b})^*$  channels, respectively. Besides, resonance ones are of 19087 MeV and 19093 MeV.

Through considering the two channels coupling, a deeper bound state which mass is 18046 MeV is obtained and the resonance state is found at 19067 MeV. The bottom part of Table XIV shows the components of these two states which the diquark-antidiquark channel  $(bb)^*(\bar{b}\bar{b})^*$  are both around 80%. Moreover, the structures of these two exotic states presented in Table XV confirm the nature of compact multiquark systems again and the calculated distances of any pair of quarks ( $\sim 0.16$  fm and 0.25 fm for bound and resonance state, respectively) are comparable with those of  $0^+$  case.

Additionally, the bound and resonance states at 18.05 GeV and 19.07 GeV, respectively are confirmed in the complex analysis. Their properties are the same as those obtained before, and both  $\sim 16$  MeV higher than  $bb\bar{b}\bar{b}$  tetraquarks in  $0^+$  states.

**The  $I(J^P) = 0(2^+)$  channel:** There are also two channels in this quantum state: one meson-meson configuration  $\Upsilon\Upsilon$ , and one diquark-antidiquark structure  $(bb)^*(\bar{b}\bar{b})^*$ . Firstly, in the single channel calculation towards these two configurations listed in Table XVI, one bound and one resonance state are both found. In particular, bound states with a nearly degenerate masses in 18238 MeV and 18241 MeV are obtained in  $\Upsilon\Upsilon$  and  $(bb)^*(\bar{b}\bar{b})^*$  channels, respectively. They are confined by  $\sim 700$  MeV binding energies. Meanwhile, the resonance masses of them are both about 19.21 GeV.

With a complete coupled-channels computation performed, masses of the bound and resonance states depressed dozen MeV. Evidently, the coupled mass of

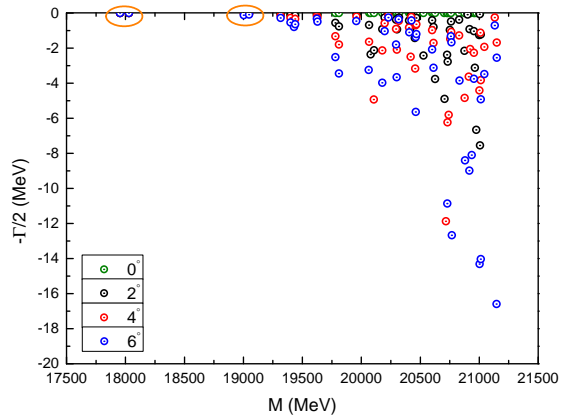


FIG. 5. Complex energies of fully-bottom tetraquarks with  $IJ^P = 00^+$  in the coupled channels calculation,  $\theta$  varying from  $0^\circ$  to  $6^\circ$ .

TABLE XIV. Possible bound and resonance states of fully-bottom tetraquarks with quantum numbers  $IJ^P = 01^+$ . The first column shows the allowed channels and, in the parenthesis, the noninteracting meson-meson threshold values. Meson-meson and diquark-antidiquark channels are indexed in the second column respectively, the third column refers to the theoretical mass of each channels and their couplings, binding energies of the dimeson channels are listed in the last column, unit in MeV. The component of each channels for bound and resonance states are listed in the bottom.

Channel	Index	$M$	$E_b$
$\eta_b \Upsilon(18864)$	1	$18062^{1st}$	-802
		$19087^{2nd}$	+223
$(bb)^*(\bar{b}\bar{b})^*$	3	$18065^{1st}$	
		$19093^{2nd}$	
Mixed		$18046^{1st}$	
		$19067^{2nd}$	
Component (1;3) <sup>1st</sup> : 16.8%; 83.2%			
Component (1;3) <sup>2nd</sup> : 23.8%; 76.2%			

TABLE XV. The distances, between any two quarks of the found fully-bottom bound and resonance states with  $IJ^P = 01^+$  in coupled-channels calculation, unit in fm.

	$r_{bb}$	$r_{\bar{b}\bar{b}}$	$r_{\bar{b}b}$
1st	0.168	0.162	0.168
2nd	0.265	0.245	0.265

bound state 18.22 GeV is extremely consistent with the announcements of CMS and RHIC collaborations [30–33], and the nature of compact diquark-antidiquark

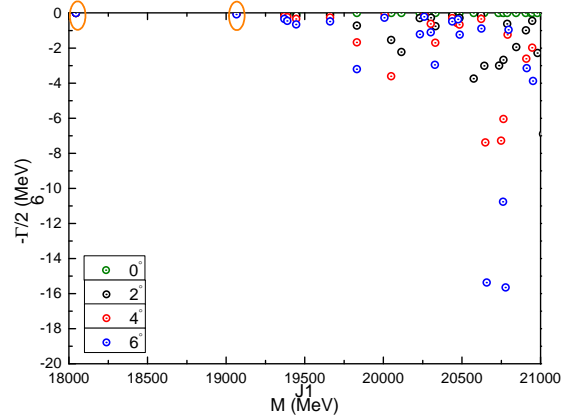


FIG. 6. Complex energies of fully-bottom tetraquarks with  $IJ^P = 01^+$  in the coupled channels calculation,  $\theta$  varying from  $0^\circ$  to  $6^\circ$ .

TABLE XVI. Possible bound and resonance states of fully-bottom tetraquarks with quantum numbers  $IJ^P = 02^+$ . The first column shows the allowed channels and, in the parenthesis, the noninteracting meson-meson threshold values. Meson-meson and diquark-antidiquark channels are indexed in the second column respectively, the third column refers to the theoretical mass of each channels and their couplings, binding energies of the dimeson channels are listed in the last column, unit in MeV. The component of each channels for bound and resonance states are listed in the bottom.

Channel	Index	$M$	$E_b$
$\Upsilon \Upsilon(18926)$	1	$18238^{1st}$	-688
		$19207^{2nd}$	+281
$(bb)^*(\bar{b}\bar{b})^*$	2	$18241^{1st}$	
		$19211^{2nd}$	
Mixed		$18223^{1st}$	
		$19189^{2nd}$	
Component (1;2) <sup>1st</sup> : 18.3%; 81.7%			
Component (1;2) <sup>2nd</sup> : 24.8%; 75.2%			

structure is established in Table XVI and XVII where the components and inner structures are investigated. Furthermore, Fig. 7 presents the distribution of complex energies in full coupled-channels computation, the obtained bound and resonance states are stable and independent of the angle  $\theta$ . Hence, the resonance state with mass of 19.19 GeV is also expected to be confirmed in future experiment. If so, the compact exotic structure, diquark-antidiquark according to our study in Table XVII can help improve our understandings to the QCD theory.

TABLE XVII. The distances, between any two quarks of the found fully-bottom bound and resonance states with  $IJ^P = 02^+$  in coupled-channels calculation, unit in fm.

	$r_{bb}$	$r_{b\bar{b}}$	$r_{\bar{b}\bar{b}}$
1st	0.174	0.168	0.174
2nd	0.271	0.251	0.271

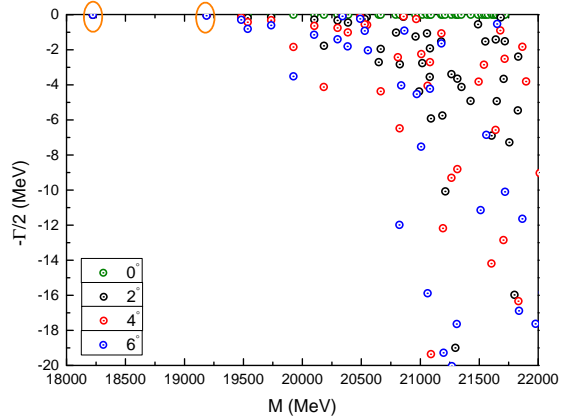


FIG. 7. Complex energies of fully-bottom tetraquarks with  $IJ^P = 02^+$  in the coupled channels calculation,  $\theta$  varying from  $0^\circ$  to  $6^\circ$ .

#### IV. EPILOGUE

The fully-heavy tetraquarks  $QQ\bar{Q}\bar{Q}$  ( $Q = c, b$ ) with spin-parity  $J^P = 0^+, 1^+$  and  $2^+$ , and in the iso-scalar sector  $I = 0$  are systemically investigated by means of a complex scaling range of potential model which is based on the results of Lattice QCD investigations on the interaction of heavy quark pair. In particular, the Cornell potential along with a spin-spin dependent interaction are included. Furthermore, the 4-body bound state issue are implemented with an extremely accurate computation approach, the Gaussian expansion method. Both meson-meson and diquark-antidiquark configurations along with their couplings are considered. The single channel calculations in each quantum state are performed firstly. Then the inner structures and components of possible bound and resonance state in the complete coupled-channels study are analyzed by computing the distances between any pair of quarks and the contributions of each channel's wave functions.

Table XVIII summarized our calculation results for the fully-heavy tetraquark in all quantum state. Firstly, no bound state is found in the fully-charm sector. However, several resonances are available in each  $J^P = 0^+, 1^+$  and  $2^+$  states, the resonance masses are listed in the parentheses. Generally, these resonance states are  $\sim 0.6$  GeV higher than the lowest noninteracting  $\eta_c\eta_c$  thresh-

TABLE XVIII. Possible bound and resonance states of fully-heavy tetraquarks. Their theoretical masses in dimeson or diquark-antidiquark ( $DA_Q$ ,  $Q = c, b$ ) channels are listed in the third column of the parentheses and the coupled results are in the last one, unit in MeV.

	$IJ^P$	Channel	Mixed	
Bound state	$00^+$	$\eta_b\eta_b$ (17999)		
		$\Upsilon\Upsilon$ (18038)		
		$DA_c^1$ (18068)	17955 <sup>1st</sup>	
		$DA_c^2$ (17975)	18030 <sup>2nd</sup>	
		$01^+$	$\eta_b\Upsilon$ (18062)	
		$DA_c$ (18065)	18046	
Resonance state	$00^+$	$\Upsilon\Upsilon$ (18238)		
		$DA_c$ (18241)	18223	
		$01^+$	$\eta_c J/\psi$ (6671)	
		$DA_c$ (6674)	6657	
		$\eta_b\Upsilon$ (19087)		
		$DA_b$ (19093)	19067	
Resonance state	$02^+$	$J/\psi J/\psi$ (7030)		
		$DA_c$ (7026)	7022	
		$\Upsilon\Upsilon$ (19207)		
		$DA_b$ (19211)	19189	
		$00^+$	$\eta_c\eta_c$ (6536)	
		$J/\psi J/\psi$ (6657)		
Resonance state	$00^+$	$DA_c^1$ (6683)	6449 <sup>1st</sup>	
		$DA_c^2$ (6469)	6659 <sup>2nd</sup>	
		$\eta_b\eta_b$ (19036)		
		$\Upsilon\Upsilon$ (19069)		
		$DA_b^1$ (19097)	19005 <sup>1st</sup>	
		$DA_b^2$ (19033)	19049 <sup>2nd</sup>	
Resonance state	$01^+$	$\eta_c J/\psi$ (6671)		
		$DA_c$ (6674)	6657	
		$\eta_b\Upsilon$ (19087)		
		$DA_b$ (19093)	19067	
		$02^+$	$J/\psi J/\psi$ (7030)	
		$DA_c$ (7026)	7022	
Resonance state	$02^+$	$\Upsilon\Upsilon$ (19207)		
		$DA_b$ (19211)	19189	

old value. In the complete coupled-channels calculations, the majority contributions (at least 60%) of these resonance states come from the diquark-antidiquark channels and they are the natures of compact tetraquark configurations with inner sizes less than 0.39 fm in all quantum states. Particularly, the obtained resonance masses in  $0^+, 1^+$  and  $2^+$  states with the complete coupled-channels computations are 6449 MeV, 6659 MeV, 6657 MeV and 7022 MeV, respectively.

As for the fully-bottom tetraquark sector, both bound and resonance states are found in  $J^P = 0^+, 1^+$  and  $2^+$ . In particular, masses of the possible bound states of  $bb\bar{b}\bar{b}$  tetraquarks in  $0^+$  and  $1^+$  states are  $\sim 18.0$  GeV. The  $2^+$  state is 200 MeV higher with the calculated mass of 18.2 GeV, and this is consistent with the announcements of CMS and RHIC collaborations [30–33]. Their binding energies are located in the energy region from 0.7 GeV to 0.9 GeV and the inner structures are quite compact within

0.18 fm. Nevertheless, extensive investigations both on experimental and theoretical sides are still necessary to verify the existence of these tightly bound states. Additionally, the obtained resonances in  $0^+$ ,  $1^+$  and  $2^+$  states are all at  $\sim 19.1$  GeV and about 0.25 GeV above the corresponding noninteracting meson-meson threshold values. The compact configurations with their sizes less than 0.27 fm is also confirmed in our investigation.

Accordingly, the obtained bound and resonance with compact configurations in fully-heavy tetraquark states can be investigated in future experiment, *e.g.*, in the ATLAS, CMS and LHCb experiments. In particular, CMS has comparable momentum and mass resolutions as LHCb, besides this collaboration has already collected

20 times more data when comparing with LHCb. Theoretically, this extreme non-relativistic system of  $QQ\bar{Q}\bar{Q}$  tetraquark is also an excellent site in confirming the validity of Lattice QCD results in multi-quark systems.

## ACKNOWLEDGMENTS

G. Yang would like to thank J. X. Zhao for the constructive discussions. The authors thank the support by Tsinghua University Initiative Scientific Research Program. Work partially financed by: National Natural Science Foundation of China under Grant Nos. 11775118, 11535005, 11975010, 11775123 and 11890712.

- 
- [1] R. Aaij *et al.* (LHCb Collaboration), Phys. Rev. Lett. **118**, 182001 (2017).
- [2] R. Aaij *et al.* (LHCb Collaboration), Phys. Rev. Lett. **124**, 082002 (2020).
- [3] R. Aaij *et al.* (LHCb Collaboration), Phys. Rev. Lett. **123**, 152001 (2019).
- [4] R. Aaij *et al.* (LHCb Collaboration), (2020), arXiv: 2002.05112 [hep-ex].
- [5] A. M. Sirunyan *et al.* (CMS Collaboration), Phys. Lett. B **803**, 135345 (2020).
- [6] R. Aaij *et al.* (LHCb Collaboration), Phys. Rev. Lett. **124**, 222001 (2020).
- [7] H. X. Chen, Q. Mao, W. Chen, A. Hosaka, X. Liu and S. L. Zhu, Phys. Rev. D **95**, 094008 (2017).
- [8] M. Karliner and J. L. Rosner, Phys. Rev. D **95**, 114012 (2017).
- [9] K. L. Wang, L. Y. Xiao, X. H. Zhong, and Q. Zhao, Phys. Rev. D **95**, 116010 (2017).
- [10] G. Yang and J. L. Ping, Phys. Rev. D **97**, 034023 (2018).
- [11] M. Karliner and J. L. Rosner, (2020), arXiv: 2005.12424 [hep-ph].
- [12] H. X. Chen, E. L. Cui, A. Hosaka, Q. Mao and H. M. Yang, Eur. Phys. J. C **80**, 256 (2020).
- [13] Z. G. Wang, Int. J. Mod. Phys. A **35**, 2050043 (2020).
- [14] L. Y. Xiaom K. L. Wang, M. S. Liu and X. H. Zhong, Eur. Phys. J. C **80**, 279 (2020).
- [15] W. H. Liang and E. Oset, Phys. Rev. D **101**, 054033 (2020).
- [16] K. Azizi and Y. Sarac and H. Sundu, (2020), arXiv: 2005.06772 [hep-ph].
- [17] K.-L. Wang, Q. F. Lü and X. H. Zhong, Phys. Rev. D **100**, 114035 (2019).
- [18] B. Chen, S. Q. Luo, X. Liu and T. Matsuki, Phys. Rev. D **100**, 094032 (2019).
- [19] K. L. Wang, L. Y. Xiao and X. H. Zhong, (2020), arXiv: 2004.03221 [hep-ph].
- [20] Q. F. Lü, (2020), arXiv: 2004.02374 [hep-ph].
- [21] H. M. Yang, H. X. Chen and Q. Mao, (2020), arXiv: 2004.00531 [hep-ph].
- [22] H. Q. Zhu, N. N. Ma and Y. Huang, (2020), arXiv: 2005.02642 [hep-ph].
- [23] R. Aaij *et al.* (LHCb Collaboration), Phys. Rev. Lett. **122**, 222001 (2019).
- [24] R. Aaij *et al.* (LHCb Collaboration), Phys. Rev. Lett. **115**, 072001 (2015).
- [25] B. Aubert *et al.* (BABAR Collaboration), Phys. Rev. Lett. **95**, 142001 (2005).
- [26] S. -K. Choi *et al.* (Belle Collaboration), Phys. Rev. Lett. **100**, 142001 (2008).
- [27] T. Aaltonen *et al.* (CDF Collaboration), Phys. Rev. Lett. **102**, 242002 (2009).
- [28] M. Ablikim *et al.* (BESIII Collaboration), Phys. Rev. Lett. **110**, 252001 (2013).
- [29] V. Khachatryan *et al.* (CMS Collaboration), J. High Energ. Phys. **05**, 013 (2017).
- [30] S. Durgut, Ph. D. thesis at University of Iowa, <https://ir.uiowa.edu/etd/6411/>.
- [31] S. Durgut, APS April Meeting 2018, <http://meetings.aps.org/Meeting/APR18/Session/U09.6>.
- [32] K. Yi, Intl. J. Mod. Phys. A Vol. 33, No. 36, 1850224 (2018).
- [33] L. C. Bland *et al.* ( $A_N$ DY Collaboration), (2019), arXiv: 1909.03124 [nucl-ex].
- [34] R. Aaij *et al.* (LHCb Collaboration), J. High Energ. Phys. **10**, 086 (2018).
- [35] L. An, LHC Seminar, <https://indico.cern.ch/event/900972/>.
- [36] M.-Z. Liu, Y.-W. Pan, F.-Z. Peng, M. S. Sánchez, L.-S. Geng, A. Hosaka and M. P. Valderrama, Phys. Rev. Lett. **122**, 242001 (2019).
- [37] J. He, Eur. Phys. J. C **79**, 393 (2019).
- [38] Z.-G. Wang, Int. J. Mod. Phys. A **35**, 2050003 (2020).
- [39] Z.-H. Guo and J. A. Oller, Phys. Lett. B **793**, 144 (2019).
- [40] H. Huang, J. He and J. Ping, (2019), arXiv: 1904.00221 [hep-ph].
- [41] H. Mutuk, Chin. Phys. C **43**, 093103 (2019).
- [42] R. Zhu, X. Liu, H. Huang and C.-F. Qiao, Phys. Lett. B **797**, 134869 (2019).
- [43] M. I. Eides, V. Y. Petrov and M. V. Polyakov, (2019), arXiv: 1904.11616 [hep-ph].
- [44] X.-Z. Weng, X.-L. Chen, W.-Z. Deng and S.-L. Zhu, Phys. Rev. D **100**, 016014 (2019).
- [45] Y. Shimizu, Y. Yamaguchi and M. Harada, (2019), arXiv: 1904.00587 [hep-ph].
- [46] C. W. Xiao, J. Nieves and E. Oset, Phys. Rev. D **100**, 014021 (2019).
- [47] L. Meng, B. Wang, G.-J. Wang and S.-L. Zhu, Phys. Rev. D **100**, 014031 (2019).

- [48] C.-J. Xiao, Y. Huang, Y.-B. Dong, L.-S. Geng and D.-Y. Chen, Phys. Rev. D **100**, 014022 (2019).
- [49] X. Cao and J.-P. Dai, Phys. Rev. D **100**, 054033 (2019).
- [50] X.-Y. Wang, X.-R. Chen and J. He, Phys. Rev. D **99**, 114007 (2019).
- [51] J.-M. Richard, A. Valcarce and J. Vijande, Phys. Lett. B **790**, 248 (2019).
- [52] Q.-S. Zhou, K. Chen, X. Liu, Y.-R. Liu and S.-L. Zhu, Phys. Rev. C **98**, 045204 (2018).
- [53] F. Giannuzzi, Phys. Rev. D **99**, 094006 (2019).
- [54] G. Yang, J. Ping and J. Segovia, Phys. Rev. D **101**, 074030 (2020).
- [55] F.-L. Wang, R. Chen, Z.-W. Liu and X. Liu, Phys. Rev. D **99**, 054021 (2019).
- [56] E. J. Eichten and C. Quigg, Phys. Rev. Lett. **119**, 202002 (2017).
- [57] M. Karliner and J. L. Rosner, Phys. Rev. Lett. **119**, 202001 (2017).
- [58] E. Hernández, J. Vijande, A. Valcarce and Jean-Marc Richard, arXiv: 1910.13394 [hep-ph].
- [59] C. E. Fontoura, G. Krein, A. Valcarce and J. Vijande, Phys. Rev. D **99**, 094037 (2019).
- [60] J. Carlson, L. Heller and J. A. Tjon, Phys. Rev. D **37**, 744 (1988).
- [61] D. Ebert, R. N. Faustov, V. O. Galkin and W. Lucha, Phys. Rev. D **76**, 114015 (2007).
- [62] G. Yang, J. Ping and J. Segovia, Phys. Rev. D **101**, 014001 (2020).
- [63] L. Leskovec, S. Meinel, M. Pflaumer and M. Wagner, Phys. Rev. D **100**, 014503 (2019).
- [64] A. Francis, R. J. Hudspith, R. Lewis and K. Maltman, Phys. Rev. Lett. **118**, 142001 (2017).
- [65] P. Junnarkar, N. Mathur and M. Padmanath, Phys. Rev. D **99**, 034507 (2019).
- [66] S. S. Agaev, K. Azizi and H. Sundu, arXiv: 1905.07591 [hep-ph].
- [67] A. Francis, R. J. Hudspith, R. Lewis and K. Maltman, Phys. Rev. D **99**, 054505 (2019).
- [68] A. Ali, Q. Qin and W. Wei, Phys. Lett. B **785**, 605 (2018).
- [69] A. Ali, A. Ya. Parkhomenko, Q. Qin and W. Wang, Phys. Lett. B **782**, 412 (2018).
- [70] A. V. Berezhnoy, A. V. Luchinsky and A. A. Novoselov, Phys. Rev. D **86**, 034004 (2012).
- [71] A. Esposito and A. D. Polosa, Eur. Phys. J. C **78**, 782 (2018).
- [72] M. N. Anwar, J. Ferretti, F. -K. Guo, E. Santopinto and B. -S. Zou, Eur. Phys. J. C **78**, 647 (2018).
- [73] M. A. Bedolla, J. Ferretti, C. D. Roberts and E. Santopinto, arXiv: 1911.00960 [hep-ph].
- [74] Z. -G. Wang, Eur. Phys. J. C **77**, 432 (2017).
- [75] W. Chen, H. -X. Chen, X. Liu, T. G. Steele and S. -L. Zhu, Phys. Lett. B **773**, 247 (2017).
- [76] Y. Bai, S. Lu and J. Osborne, Phys. Lett. B **798**, 134930 (2019).
- [77] C. Becchi, A. Giachino, L. Maiani and E. Santopinto, arXiv: 2002.11077 [hep-ph].
- [78] W. Heupel, G. Eichmann and C. S. Fischer, Phys. Lett. B **718**, 545 (2012).
- [79] V. R. Debastiani and F. S. Navarra, Chin. Phys. C **43**, 013105 (2019).
- [80] A. V. Berezhnoy, A. K. Likhoded, A. V. Luchinsky and A. A. Novoselov, Phys. Rev. D **84**, 094023 (2011).
- [81] M. Karliner, S. Nussinov and J. L. Rosner, Phys. Rev. D **95**, 034011 (2017).
- [82] K. Yi, Intl. J. Mod. Phys. A Vol. 28, No. 18 (2013) 1330020.
- [83] J. -M. Richard, A. Valcarce and J. Vijande, Phys. Rev. D **95**, 054019 (2017).
- [84] J. Wu, Y. -R. Liu, K. Chen, X. Liu and S. -L. Zhu, Phys. Rev. D **97**, 094015 (2018).
- [85] M. S. Liu, F. X. Liu, X. H. Zhong and Q. Zhao, arXiv: 2006.11952 [hep-ph].
- [86] X. Chen, Eur. Phys. J. A **55**, 106 (2019).
- [87] M. -S. Liu, Qi -F. Lü and X. -H. Zhong and Q. Zhao, Phys. Rev. D **100**, 016006 (2019).
- [88] G. -J. Wang, L. Meng and S. -L. Zhu, arXiv: 1907.05177 [hep-ph].
- [89] J. -M. Richard, A. Valcarce and J. Vijande, Phys. Rev. C **97**, 035211 (2018).
- [90] C. Hughes, E. Eichten and C. T. H. Davies, Phys. Rev. D **97**, 054505 (2018).
- [91] G. Yang and J. Ping, Phys. Rev. D **95**, 014010 (2017).
- [92] E. Hiyama, Y. Kino and M. Kamimura, Prog. Part. Nucl. Phys. **51**, 223 (2003).
- [93] T. Kawanai and S. Sasaki, Phys. Rev. D **85**, 091503 (2012).
- [94] C. Alexandrou, Ph. de Forcrand and O. Jahn, Nucl. Phys. B **119**, 667 (2003).
- [95] J. Zhao, K. Zhou, S. Chen and P. Zhuang, arXiv: 2005.08277 [nucl-th].
- [96] J. Aguilar and J. M. Combes, Commun. Math. Phys. **22**, 269 (1971).
- [97] E. Balslev and J. M. Combes, Commun. Math. Phys. **22**, 280 (1971).
- [98] M. Harvey, Nucl. Phys. A **352**, 326 (1981).
- [99] J. Vijande, A. Valcarce and N. Barnea, Phys. Rev. D **79**, 074010 (2009).